

Lipid Microdomain-Dependent Macropinocytosis Determines Compartmentation of *Afipia felis*

Bianca Schneider¹, Christian Schueller¹,
Olaf Utermohlen² and Albert Haas^{1,*}

¹Institute for Cell Biology, University of Bonn,
Ulrich-Haberland-Strasse 61a, 53121 Bonn, Germany

²Institute for Medical Microbiology, Immunology, and
Hygiene, Köln University, Goldenfelsstrasse 29-31,
50935 Köln, Germany

*Corresponding author: Albert Haas,
albert.haas@uni-bonn.de

Phagocytic compartments are specialized endocytic organelles and usually mature along the degradative pathway into phagolysosomes. The rare human pathogen *Afipia felis* localizes to a compartment that is different from canonical phagocytic compartments. Here, we present evidence that internalization of *Afipia* by macrophages and unusual phagosome development are considerably decreased by attachment of cholera toxin B subunit to macrophage ganglioside GM1 or by extraction or oxidation of plasma membrane cholesterol. Amiloride (an inhibitor of Na⁺/H⁺ exchanger and macropinocytosis) strongly inhibited uptake of *A. felis* at a late step, i.e. the closure of macropinocytic structures rather than the production of membrane ruffles. Ultrastructural evidence showed that *A. felis* was taken up by macrophages via macropinocytosis. In contrast, *A. felis* opsonized with a monoclonal IgG antibody was ingested by a zipper-like mechanism, resulting in normal phagosome maturation. Hence, while the preferred path of *A. felis* uptake is dependent on the integrity of lipid microdomains and on macropinocytosis, and while this uptake leads to an unusual phagosome and to intracellular survival of *A. felis*, those bacteria that enter using Fcγ receptors are delivered to a late endocytic compartment.

Key words: endosome, lysosome, macropinocytosis, phagocytosis, phagosome, pathogen, macrophage, immunity, compartments, intracellular

Received 10 July 2006, revised and accepted for publication 8 December 2006

The plasma membrane is the boundary between the worlds within and outside the cell and is the contact surface with which a pathogen interacts when it enters a cell. Particle ingestion (phagocytosis) requires comprehensive actin rearrangements beneath the plasma membrane and leads to the creation of a new cytoplasmic organelle, the phagosome, a specialized form of an endosome (1,2). A phagosome normally passes through a set of defined steps in a process termed phagosome maturation, and develops into a strongly acidic phagolysosome. In this

organelle, bacteria are killed and digested and antigens may be presented via MHCII molecules. A particular group of pathogens, the 'intracellular' pathogens, however, escape killing and degradation (1,2). One of these pathogens is *Afipia felis*, a rare cause of human cat scratch disease (3,4) and an interesting model for unusual phagosome maturation.

Most of the *A. felis*-containing vacuoles (ACVs) are phagosomes that, at 2 h of infection, contain neither of a dozen 'classical' early and late endosome proteins nor the endoplasmic reticulum marker calnexin or Golgi GM130 (5,6). In contrast, a minor proportion of *Afipia* will finally be localized to phagolysosomes, and phagosomes containing these few *Afipiae* are positive for the early endosomal protein EEA1 in the first minutes of infection, then quickly loose the marker and do localize to phagolysosomes (6). These findings suggested that entry of *A. felis* after binding a particular set of surface receptors might lead to the establishment of an unusual (i.e. not destined for degradation) phagosome. This is reminiscent of the situation with *Escherichia coli* which ligates macrophage CD48 via the bacterial lectin FimH leading to non-acidified phagosomes (7). When the same bacteria had been opsonized with specific antibodies and were thus forced to enter via high-affinity Fcγ receptors, they were delivered to an acidic compartment, the composition of which has not been investigated. Detergent-resistant membrane lipid microdomains, also called 'lipid rafts', seemed to be involved in the unusual localization of *E. coli* (7).

Such membrane lipid microdomains are small specialized membrane areas containing high concentrations of saturated (glyco)sphingolipids, cholesterol, glycosylphosphatidylinositol (GPI)-anchored or double-acylated proteins (8,9). A certain set of transmembrane and peripheral membrane proteins is permanently associated with such microdomains, others can segregate into these microdomains under certain conditions, e.g. after receptor ligation. Lipid microdomains are dynamic signaling platforms which, once their signaling proteins are activated, tend to coalesce and can then transduce signals from the outside into the cell (9). Activated lipid microdomains can organize cellular machineries, e.g. assemble actin filaments and, the other way around, are themselves stabilized by actin organizers such as Rac/Rho, hinting at a cross-talk between lipid microdomains and cytoskeletal elements (10).

Binding to and entering of mammalian cells by several pathogens can be disturbed experimentally by reagents that alter cholesterol content or chemistry (7,11–14).

These studies were very suggestive in what concerns the possible involvement of lipid microdomains in pathogen binding and entry. However, they did not follow up on the compartmentation of phagosomes containing those bacteria that were forced to enter differently than through the lipid microdomain-associated port of entry.

A connection between lipid microdomain engagement by *Brucella abortus* and its uptake by macropinocytosis, rather than by conventional phagocytosis, has been reported (15). Macropinocytosis is a cellular process to ingest large samples of environmental fluid, initially producing large vacuoles (0.2–5 μm in diameter) which often shrink quickly (16). Macropinocytosis occurs constitutively in professionally phagocytic macrophages and, in particular, dendritic cells (17), yet requires stimulation in non-professionally phagocytic cells, e.g. in epithelial cells by growth hormones (18). Macropinocytosis can be readily analyzed experimentally by inclusion of large bulk-phase markers, such as 70 000 MW dextran which is not well incorporated into small clathrin-coated vesicles (19).

The experiments in this study demonstrate that *A. felis* usually enters murine macrophages through a macropinocytic process that requires an intact lipid microdomain environment. We further show that usage of this pathway is required for the establishment of an ACV that lacks typical features of the degradative phagocytic pathway and allows bacterial survival inside macrophages.

Results

Afipia felis uptake in J774E is slow and accompanied by reduced actin polymerization

When uptake of *A. felis* into macrophage-like cells was observed microscopically, it seemed to be unusually slow. Hence, we followed the kinetics of *Afipia* internalization. J774E were infected with either mock-treated *A. felis* or *A. felis* coated with specific IgG to *A. felis* lipoprotein. At various times, macrophages were fixed and a differential antibody staining was performed to distinguish between intra- and extracellular bacteria. *Afipia felis* coated with monoclonal IgG were used as a control, as this treatment provides a high-affinity ligand for Fc γ receptors on the macrophage surface and normalizes phagosome maturation compared to mock-treated bacteria (4). Uptake of IgG-opsionized *A. felis* was very fast with some 90% of the bacteria being internalized by 10 min post-infection. Non-opsionized *Afipia* were taken up much slower with only approximately 40% being intracellular at 60 min (Figure 1A).

To test whether uptake depended on the actin cytoskeleton, macrophages were treated with cytochalasin D to inhibit actin polymerization. This treatment reduced uptake of non-opsionized or opsionized *Afipia* by 85 or 91%, respectively, indicating that phagocytosis is actin dependent in either case (data not illustrated). However, filamentous

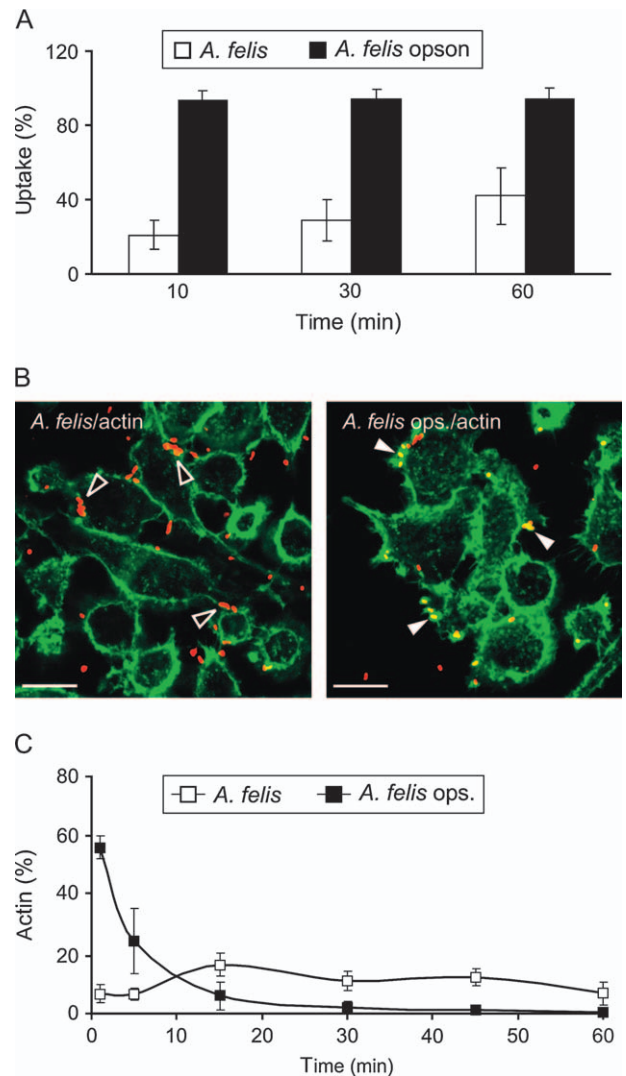


Figure 1: Uptake of *A. felis* by macrophages is slow and accompanied by reduced actin polymerization. A) Uptake of *A. felis* or antibody-coated *A. felis* by macrophages was determined at 10, 30 and 60 min of infection using differential inside-outside staining (data from three independent experiments \pm SD). B) J774E cells were infected with untreated or antibody-coated *A. felis* using a centrifugation step as detailed in the Materials and Methods section. Preparations were warmed for 1 min, fixed and prepared for microscopy. F-actin (phalloidin) appears in green, bacteria in red. An optical overlay is shown. While untreated bacteria do not colocalize (open arrowheads), opsionized ones do (closed arrowheads). Bar, 10 μm . C) Quantification of colocalization analyzes as in B at various times of infection (means \pm SD from three independent experiments; 200 macrophages were counted per sample and experiment). Bar, 10 μm .

actin beneath attached non-opsionized *Afipia* was rare and less abundant (Figure 1B). A maximum of 20% attached *A. felis* was positive at any time, and polymerized actin was still seen after 60 min (Figure 1C). In contrast, approximately 60% of opsionized *A. felis* were surrounded by filamentous (phalloidin-positive) actin within the first

minute of infection while after 15 min, no colocalization was detected (Figure 1B, C).

Opsonization of *A. felis* normalizes phagosome biogenesis

Opsonization not only results in increased and faster ingestion of *Afipia* (see above) but also in more frequent phagolysosome formation (4). Here, J774E cells were infected with opsonized or non-opsonized *Afipia* as above, the infection chased for various times, and colocalization of the bacteria with the transferrin receptor (TfR) was quantified. A strong and frequent colocalization of TfR, a paradigm resident protein of non-raft plasma membrane domains (20,21), with opsonized *A. felis* was observed (Figure 2A, B). Phagosomes containing non-opsonized *A. felis*, however, colocalized only extremely rarely at any time investigated (Figure 2A, B). This exclusion of a non-raft marker present in most early phagosomes (22–24) further strengthened our previous notion that biogenesis of *A. felis*-containing phagosomes is non-canonical starting from the moment of ingestion.

Finally, to kinetically dissect the accessibility of ACVs for endocytic tracers, J774E cells were infected for various times with either *A. felis*, opsonized *A. felis* or heat-killed *A. felis* and subsequently chased with medium containing 10 000 MW dextran Texas Red (DTxR) for 2 h. There was substantial colocalization (~70%) with heat-killed *A. felis* already at 30 min of infection. A gradually increasing percentage of DTxR-positive phagosomes containing opsonized live *A. felis* was also observed (~40% at 2 h), while the percentage of DTxR-positive phagosomes containing non-opsonized *A. felis* was less than 20% at all times tested (Figure 2C). In summary, only very few unopsonized bacteria entered J774E cells through a pathway positive for TfR and also very few bacteria were contained in the degradative pathway, suggesting that these two pathways were linked.

Membrane domains rich in GM1 and cholesterol facilitate *Afipia* uptake by J774E

Recent studies have highlighted a role of lipid microdomains as signaling platforms in the entry of several micro-organisms into host cells [reviewed by Duncan et al. (25) and Manes et al. (26)]. Such microdomains do not possess TfR. We therefore investigated their role in the entry of *A. felis* by treating cells with the non-toxic pentameric cholera toxin B subunit (CTB). CTB ligates the ganglioside GM1, a glycolipid which is accumulated in lipid microdomains. CTB affinity for GM1 is particularly high when the glycolipid is complexed in lipid rafts (8,14,27,28). After treatment with CTB for 30 min at 37°C, macrophages were infected with either *A. felis*, opsonized *A. felis*, or *E. coli* for 90 min, followed by a 1 h chase in the presence of gentamicin to kill extracellular bacteria and by determination of the number of intracellular (gentamicin-protected) bacteria. When J774E cells were pretreated with CTB, uptake of *Afipia* into J774E cells was

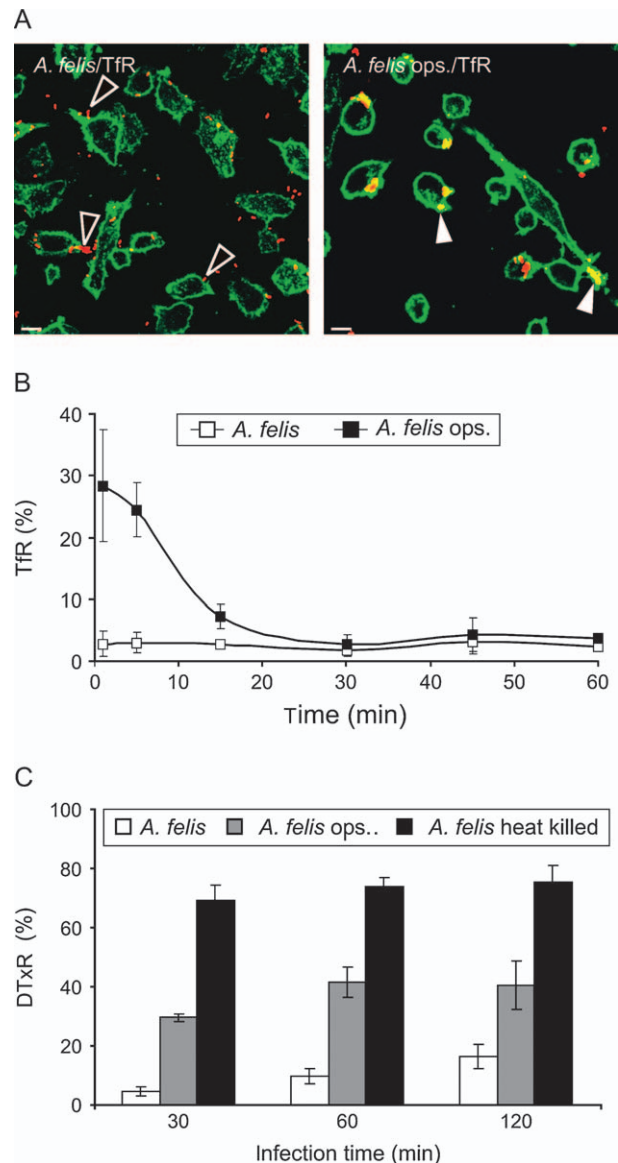


Figure 2: Interaction of phagosomes with early endocytic compartments. A) J774E macrophages were infected with either untreated or antibody-coated ('ops.') *A. felis* as in Figure 1. After 1 min of infection, samples were fixed and stained for bacteria (red) and TfR (green). An optical overlay is shown. Note that phagosomes containing opsonized bacteria are positive for TfR (closed arrowheads), while non-opsonized bacteria were not (open arrowheads). Bar, 10 μ m. B) Quantification from data obtained in kinetic experiments as in A using confocal microscopy (means \pm SD from three independent experiments, 200 macrophages were counted per sample and experiment). C) J774E cells were infected with either *A. felis* or opsonized *A. felis* as in Figure 1 and phagosomes were allowed to mature for 30, 60 or 120 min. A 2-h incubation with fresh medium containing 0.15 mg/mL DTxR 10 000 MW followed. Colocalization of bacteria with DTxR was quantified. Data from three independent experiments with means and SD are shown; 200 macrophages were counted per sample and experiment.

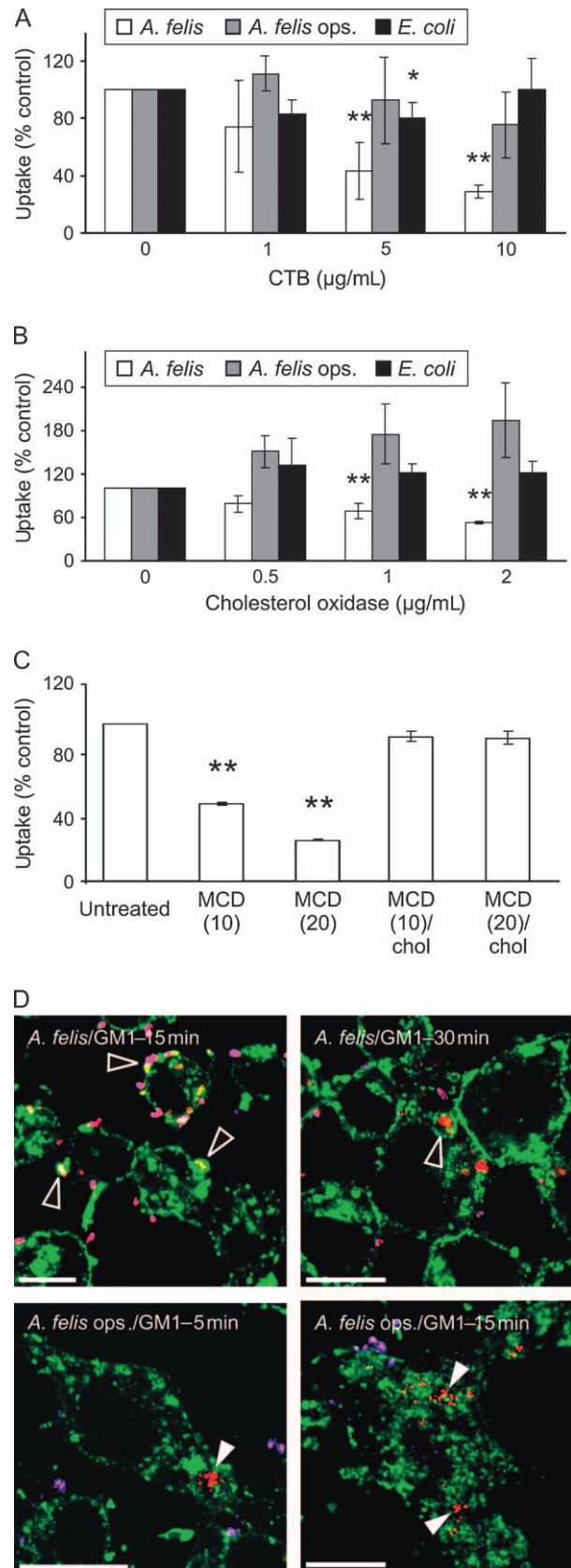
inhibited in a dose-dependent manner. In contrast, phagocytosis of opsonized *Afipia* or *E. coli* was not affected (Figure 3A). Nicely fitting with these observations, confocal immunofluorescence revealed that CTB strongly labeled newly formed phagosomes containing non-opsonized, but not opsonized, bacteria (Figure 3D).

To further test whether internalization of *Afipia* occurred via lipid microdomains, we pretreated macrophages with either cholesterol oxidase (Figure 3B) or methyl- β -cyclodextrin (MCD; Figure 3C). MCD, a water-soluble cyclic oligosaccharide (29), can physically extract most cholesterol from cell membranes and, hence, disrupt raft cohesion (see also Figure 4B). Oxidation of cholesterol by cholesterol oxidase to cholestenone breaks the hydrogen-bonding patterns of cholesterol hydroxyl groups with sphingolipid amido groups (30,31), hence destroying the coherent forces in lipid microdomains and disrupting their integrity and signaling functions. Here, treatment with cholesterol oxidase resulted in significantly decreased uptake of *A. felis* by J774E cells, whereas uptake of *E. coli* was not affected and uptake of opsonized *Afipia* was even increased (Figure 3B). As cholesterol has a significant ordering effect on membrane lipid acyl chains, oxidation of cholesterol might decrease membrane fluidity and rigidity (32) and could enhance phagosome formation when this is not directly dependent on lipid microdomain integrity. Fc γ -receptor-mediated uptake could, under these circumstances, be further increased.

Treatment with MCD also clearly reduced uptake of *A. felis* (Figure 3C), but not of opsonized *Afipia* or of *E. coli* (data not illustrated). As MCD not only extracts cholesterol from membranes, but may also extract complex fatty acids (33) and likely other compounds, we replenished membrane cholesterol by adding pre-formed cholesterol-MCD complexes to previously cholesterol-extracted macrophages (20,34). This treatment restored the ability to ingest non-opsonized *Afipia* to the level of untreated cells (Figure 3C).

Figure 3: Uptake of *A. felis* is inhibited by treatment of macrophages with CTB, cholesterol oxidase or MCD.

Untreated control J774E macrophages or macrophages pretreated with indicated concentrations of A) CTB, B) cholesterol oxidase or C) 10 or 20 mM MCD were incubated with *A. felis* (MOI 200; open symbols), opsonized *A. felis* (MOI 50; gray symbols) or *E. coli* (MOI 100; black symbols) for 90 min, followed by gentamicin protection assays to quantify ingested bacteria. Alternatively, after treatment with MCD, macrophages were incubated in medium containing MCD-cholesterol complexes to replenish host cell plasma membrane cholesterol before infection, as indicated. Data shown are percent intracellular bacteria relative to untreated control cells (means \pm SD from three independent experiments). Significances were * $p < 0.05$; ** $p < 0.01$). D) J774E cells were infected with untreated (open arrowheads) or antibody-coated *A. felis* (closed arrowheads) after a centrifugation step as detailed in the Materials and Methods section. Preparations were warmed, fixed at the indicated times and prepared for microscopy using fluorescent CTB. GM1 appears in green, and bacteria in red. An optical overlay is shown. Bars, 10 μ m.



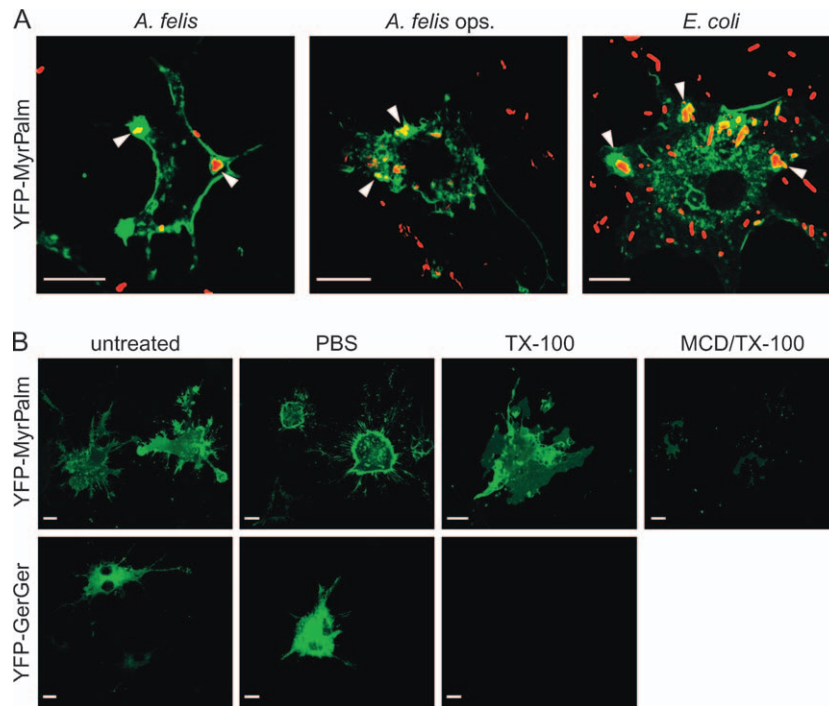


Figure 4: YFP-MyrPalm is found in TX-100-resistant membrane domains and on all phagosomes. A) RAW 264.7 macrophages transfected with a plasmid expressing YFP-MyrPalm were infected for 5 min with *A. felis* (MOI 100), opsonized *A. felis* (MOI 10) or *E. coli* (MOI 50) after a centrifugation step as detailed in the Materials and Methods section. Bacteria appear in red, and YFP-MyrPalm in green. Note that all particles colocalize with YFP-MyrPalm. Arrowheads denote positive phagosomes. Optical overlays are shown. B) RAW 264.7 macrophages were transfected with either the YFP-MyrPalm (upper panel) or the YFP-GerGer (lower panel) construct and cultivated for 1 day. Samples were either left untreated or were treated for 30 min with only ice-cold PBS (PBS), ice-cold PBS/1% TX-100 (TX-100) or 20 mM MCD and then extracted with ice-cold PBS/1% TX-100 (MCD/TX-100). All samples were fixed and prepared for confocal fluorescence microscopy. Micrographs show representative cells ('YFP-GerGer + TX-100' shows an arbitrary field, as all fluorescence was extracted). Bar, 10 μm .

Visualization of lipid microdomains

To analyze with optical methods whether there is involvement of lipid microdomains, we transiently transfected murine RAW 264.7 macrophages with short peptide fusion constructs that possess a consensus sequence either for myristoylation and palmitoylation or for geranylgeranylation, fused to yellow fluorescent protein (YFP), yielding YFP-MyrPalm and YFP-GerGer, respectively. While YFP-MyrPalm partitions into lipid raft domains, YFP-GerGer is found in non-raft membrane domains (35). Transfected macrophages were infected with either *A. felis* (opsonized or not) or *E. coli*, and colocalization with the YFP constructs was analyzed by confocal microscopy (Figure 4A). All types of phagosomes were positive for YFP-MyrPalm, indicating that lipid microdomains were incorporated into all tested phagosomes (Figure 4A). Enrichment of YFP-GerGer was not detected on any of these phagosomes (data not shown). *A. felis*-containing phagosomes excluded the non-raft TfR and, therefore, colocalization with YFP-MyrPalm could be explained by their raft content. Phagosomes containing *E. coli* did not exclude TfR (Figure 2B) but still localized to phagosome positive for YFP-MyrPalm (Figure 4A). It was therefore necessary to ascertain that the two YFP-based probes partitioned in the macrophage

membranes as expected and that it was not overexpression of YFP-MyrPalm that would make this probe appear indiscriminately in all membrane domains.

To address this question, RAW 264.7 macrophages were transiently transfected with YFP-MyrPalm and treated with a low concentration (1%) of Triton X-100 (TX-100) at 4°C followed by formaldehyde fixation. Treatment with cold TX-100 removes much of the cellular membranes, yet leaves lipid microdomains undisturbed which is a hallmark feature of such microdomains (36). Use of this method *in situ* precludes many possible artifacts that can occur during biochemical purification of microdomains (37). Cells expressing YFP-MyrPalm had an almost unaltered fluorescence pattern after TX-100 extraction, while macrophages expressing YFP-GerGer had lost their fluorescence (Figure 4B), indicating that these peptides had partitioned as expected. When macrophages expressing YFP-MyrPalm were first treated with MCD and then subjected to TX-100 treatment, most of the YFP-MyrPalm label vanished, demonstrating that our protocol for treatment with MCD effectively disrupts rafts as visualized by the changed sensitivity of YFP-MyrPalm toward TX-100 treatment. These data are in agreement with previously published

work that used fluorescence resonance energy transfer analysis with YFP-MyrPalm-transfected cells to test the utility of these YFP-based probes in raft analysis (35).

Non-opsonized *A. felis* enter by lipid-raft-dependent macropinocytosis

To study uptake of *A. felis* at the ultrastructural level, we performed transmission electron microscopy on samples of J774E macrophages that were briefly infected either with untreated or with opsonized *A. felis*. Non-opsonized *A. felis* were loosely attached to plasma membranes [Figure 5(1)] and were entangled in very long filipodial and ruffle-like structures which, at least in some cases, obviously lead to the creation of spacious bacteria-containing vacuoles [Figure 5(2A, B), (2C) open arrowhead], followed by shrinkage of micropinosomes within minutes [Figure 5(2C) closed arrowheads]. Spacious and tightly fitting vacuoles occurred within the same macrophage, with the spacious ones being usually localized to the cell periphery, presumably representing newly formed phagosomes [Figure 5(2C) open arrowhead]. Shrinking of these compartments leads to tightly fitting phagosomes, located to a perinuclear region [Figure 5(2C) closed arrowheads]. Such behavior was clearly reminiscent of macropinocytosis, which is a means of cells to ingest large quantities of liquid (38) and is used by *Salmonella* to enter macrophages by induced macropinocytosis (39). In contrast, opsonized bacteria were tightly apposed to extended plasma membrane regions, they were likely taken up via immunoglobulin receptors through zipper-like phagocytosis [Figure 5(3)] and they were delivered into tightly fitting phagosomes [Figure 5(3C)].

To further analyze whether *A. felis* is taken up by macropinocytosis, we treated macrophages with amiloride, a commonly used drug to inhibit macropinocytosis (18,40, 41). Amiloride inhibits the NHE-1 Na^+/H^+ exchanger (42) and causes to cytoplasm acidification. It is not clear at which stage of macropinocytosis amiloride and its targets act. We incubated macrophages with amiloride at 2 or 5 mM for 10 min before performing a 30-min infection (with amiloride present), followed by differential inside-outside staining and fluorescence microscopy. While opsonized *Afipia* were taken up at the same frequency regardless of whether amiloride was present or not, uptake of non-opsonized *Afipia* was considerably decreased (Figure 6A), although the number of attached bacteria was hardly reduced ($91 \pm 7.6\%$). On an ultrastructural level, amiloride led to an accumulation of filipodial and ruffle structures and only very few *A. felis* were seen inside treated macrophages [Figure 5(4)]. These data suggested that ruffle formation was unaffected by amiloride while ruffle consumption was inhibited.

To further analyze whether a macropinosome is the primary location of non-opsonized *A. felis* in J774E cells, we labeled the plasma membranes using the membrane-labeling styryl dye FM4-64 which is strongly red fluorescent

once it is integrated into membranes (43). Non-opsonized bacteria were usually ingested into large FM4-64-stained structures while opsonized *A. felis* were normally found in tight phagosomes, having approximately bacterial size (Figure 6B).

In a third type of experiment, the macropinocytic probe 70 000 MW DTxR was added together with the bacteria. Using non-opsonized bacteria, we often saw (green) bacteria at the cell periphery within a large red spot, a typical appearance of macropinosomes [Figure 6C(1), C(2)]. These very large structures typically became quickly smaller [Figure 6C(3)], similar to those described for macropinosomes containing *Francisella tularensis* [(44) note co-existing large (open arrowhead) and small (closed arrowheads) vacuoles in Figure 5(2C)]. In contrast, opsonized bacteria were never found to colocalize with this macropinocytosis probe at all [Figure 6C(4)], further supporting that macropinocytic structures are the first residence of non-opsonized *A. felis Afipia* that did not colocalize with DTxR in Figure 6C were most likely extracellular bacteria as uptake of *Afipia* is quite slow (Figure 1A) and infection was performed without an initial centrifugation step.

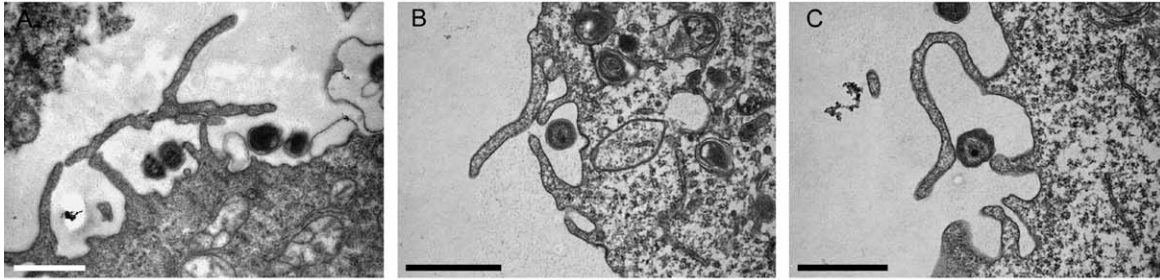
To analyze whether the uptake of the non-opsonized *Afipia* via macropinocytosis would lead to increased bacterial survival, we analyzed the number of live bacteria in macrophages by plating on nutrient agar. *Afipia felis* in untreated macrophages persisted for 24 h without much loss in viability. In amiloride-treated macrophages, however, *A. felis* was almost completely eliminated within 24 h (Figure 6D). This finding strongly suggests that macropinocytosis favors bacterial persistence inside macrophages.

Our above interpretations were based on previous reports that amiloride can indeed inhibit macropinocytosis (45) and that 70 000 MW DTxR is a specific probe for macropinocytosis (19). Therefore, we tested whether this was also true for J774E macrophage cells: when 70 000 MW DTxR was added to macrophages for 30 min, vesicular structures of various sizes and ages containing DTxR were seen throughout the cell (Figure 7, left). When DTxR was added in the presence of amiloride, few vesicular structures were detected, all of which were limited to the cell periphery and could be unconsumed pre-macropinosome structures (Figure 7, middle). Pretreatment of J774E cells with MCD almost completely eliminated the capability of these cells to ingest DTxR (Figure 7, right), suggesting that lipid microdomain integrity was crucial for this type of macropinocytosis as it is for *Afipia* uptake.

***Afipia* entry depends on phosphatidylinositol 3-kinases and dynamin-2 is not recruited**

J774E cells were treated with wortmannin, an inhibitor of type I phosphatidylinositol 3-kinases [PI(3) kinases], which inhibits macropinocytosis and phagocytosis but not uptake

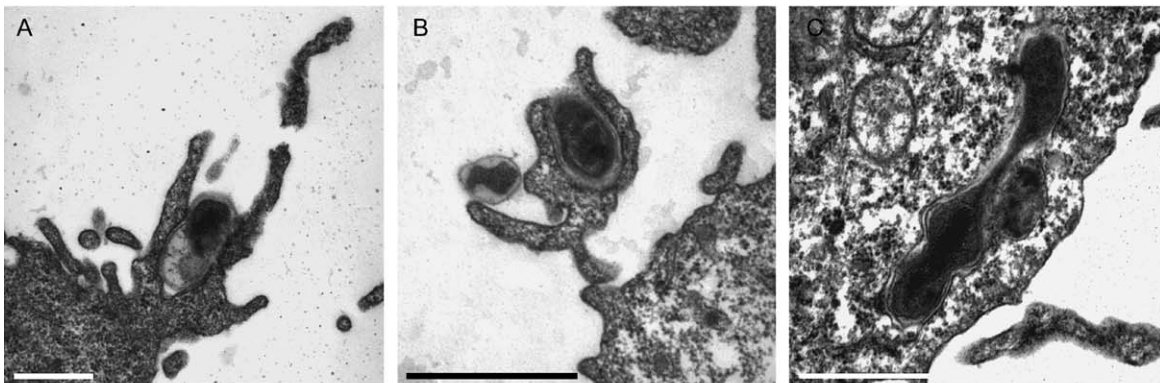
(1) *A. felis* 1 min



(2) *A. felis* 10 min



(3) *A. felis* ops. 1 min



(4) *A. felis* 10 min + amiloride

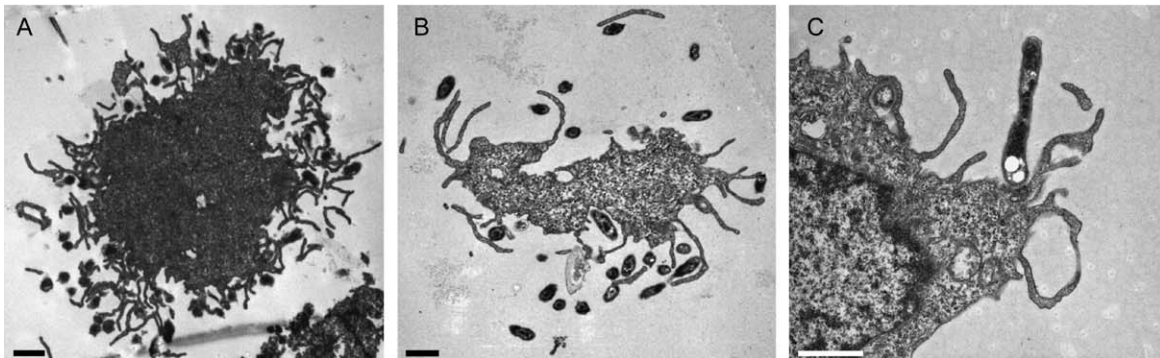


Figure 5: *Afipia felis* is taken up by macropinocytosis as analyzed by transmission electron microscopy. Transmission electron micrographs showing J774E cells infected with *A. felis* for 1 min (1) or 10 min (2, 3, 4). Bacteria were opsonized before infection with monoclonal antibody 1A5-5 (3) or not (1, 2, 4), and in (4), macrophages were incubated with 5 mM amiloride before adding *Afipia*. Closed arrowheads indicate vacuoles with tightly fitting membranes; open arrowheads indicate 'spacious' phagosomes. Bars, 1 μ m.

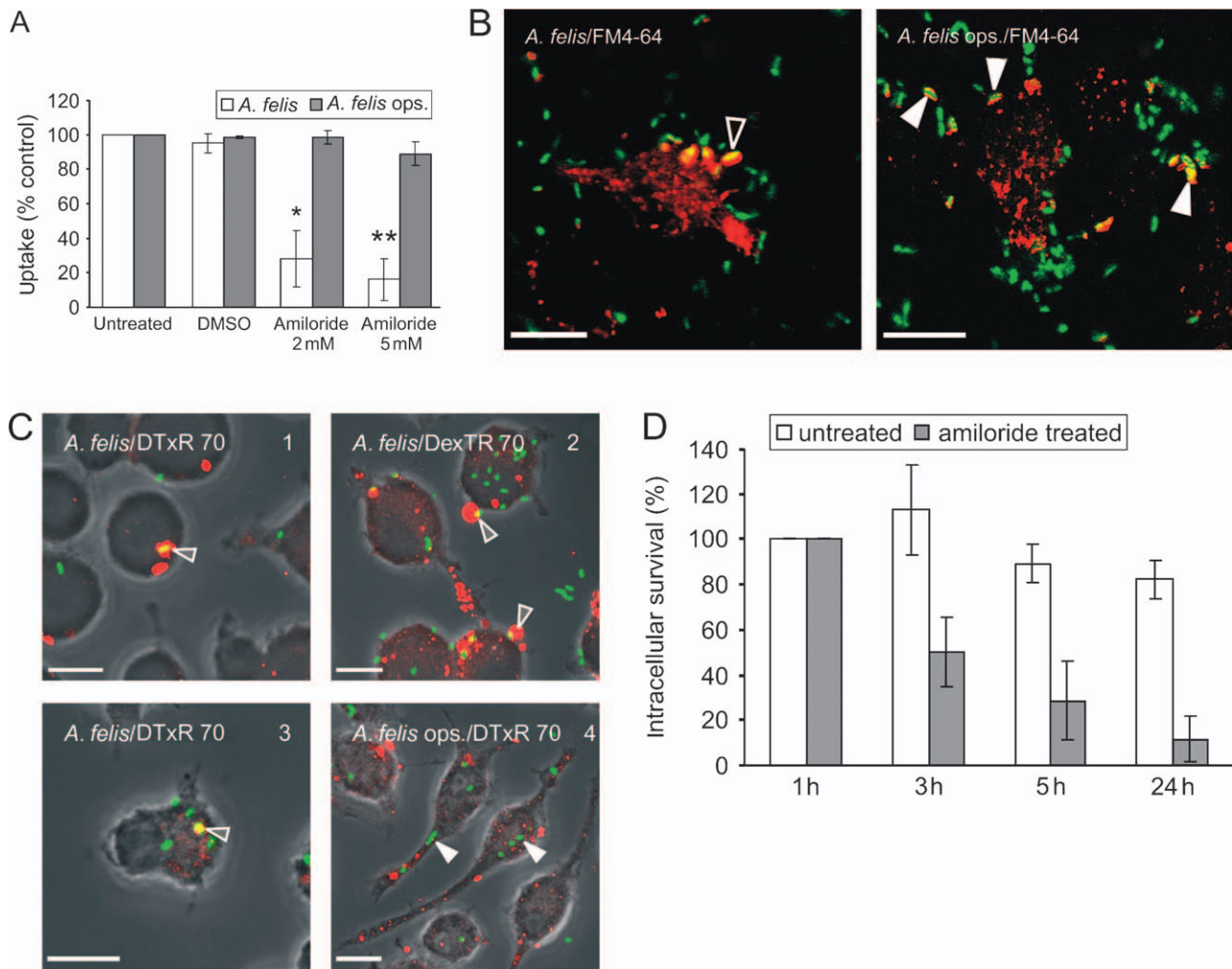


Figure 6: *Afipia felis* is taken up by amiloride-sensitive macropinocytosis. A) J774E macrophages were pretreated with amiloride (Materials and Methods section) or dimethyl sulfoxide (DMSO, carrier for amiloride) and then infected with non-opsonized or opsonized *A. felis* and uptake was quantified by differential inside–outside staining. Uptake of mock-treated ('untreated') *A. felis* was defined as 100% and relative uptake was calculated. Means \pm SD from three independent experiments with 100 macrophages counted per experiment are shown. Significances were * $p < 0.05$; ** $p < 0.01$. B) J774E cells were preincubated with the lipophilic styryl dye FM4-64 (red), unbound label was removed and macrophages were infected with *A. felis* (green) non-opsonized (left) or opsonized (right). Note that bacteria on the left are found in spacious endocytic compartments (open arrows) while green and red fluorescence are congruent in the sample on the right (closed arrows). C) Non-opsonized or opsonized *A. felis* (green) were added to J774E macrophages in the presence of 0.4 μ g/mL 70 000 MW DTxR (red). Infection was for 30 min without further chase (1, 2 and 4), or was with another 30-min chase (3). Note the very large red structures that contain non-opsonized *A. felis* (open arrowheads) with a clearly reduced size at 30 min, while opsonized bacteria (closed arrowheads) contain so little, if any, DTxR that it was not detected at these identical settings. Representative optical overlays are shown in B and C. In C, the phase-contrast images have also been overlaid. Bars, 10 μ m. D) Analysis of live cell counts in infected macrophages. J774E macrophages were infected with non-opsonized *A. felis* in the presence or absence of 5 mM amiloride for 30 min, followed by gentamicin protection assays (addition of gentamicin = 0 h). At the indicated times, cells were lysed and plated on buffered charcoal yeast extract agar plates to quantify live intracellular bacteria. Data from three independent experiments are presented with means and SD.

through caveolae (45–47). Wortmannin reduced uptake of either non-opsonized or opsonized *A. felis* by more than 80% (data not shown), as expected.

Dynamin-2 is typically found on early endosomes, early phagosomes and caveosomes (48–51). Here, opsonized *A. felis* entered into a phagosome positive for green fluorescent protein (GFP)–dynamin-2, while we never observed co-

localization of non-opsonized *A. felis* with GFP–dynamin-2 (Figure 8), as has been described for macropinosomes (52).

Entry into macrophages via lipid microdomains determines phagosome fate

While it has been shown for several models of infection that disrupting raft function can alter pathogen binding and

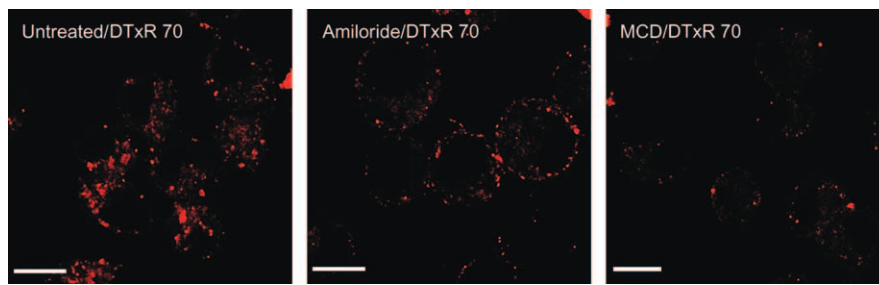


Figure 7: 70 000 MW DTxR enters J774E macrophages by amiloride-sensitive macropinocytosis. 70 000 MW DTxR was added to macrophages for 30 min in the absence (left) or presence (middle) of 5 mM amiloride, or in the absence of amiloride but after incubating the macrophages in the presence of 20 mM MCD (right). All pictures were representative and were taken with identical settings on the confocal microscope without any post-photographic signal adjustment. Bars, 10 μ m

uptake, it is not known whether those few pathogens that enter macrophages, in spite of the addition of inhibitory compounds, are still able to interfere with normal phagosome maturation. Using antibodies to lysosome-associated membrane protein-1 (LAMP1) as means to identify late phagocytic and phagolysosomal bacteria, we found that while less than 20% of *A. felis* were found in late compartments in untreated macrophages at 3 h of infection, approximately 70% of either heat-killed or opsonized bacteria were LAMP1 positive (Figure 9). Pretreatment of macrophages with either CTB or MCD increased LAMP1 colocalization from 20% to 50–60%, indicating that the trafficking pattern was normalized for many of these phagosomes. Almost identical data were obtained when lysosomes were pre-labeled with 10 000 MW DTxR and colocalization with *A. felis* was quantified (data not shown).

Discussion

In this study, we have demonstrated that non-opsonized *A. felis* enter murine macrophages through lipid microdomain-dependent macropinocytosis into an atypical phagosome while opsonized *A. felis* are delivered to a late phagocytic compartment. Evidence for the involvement of lipid microdomains was that (i) extracting cholesterol from macrophages with MCD inhibited binding and uptake of non-opsonized *A. felis* and replenishing cholesterol normalized uptake; (ii) treatment of macrophages with

cholesterol oxidase inhibited binding and uptake of non-opsonized *A. felis*; (iii) addition of CTB inhibited binding and uptake of non-opsonized *A. felis*; (iv) non-opsonized *A. felis* were routed to a non-canonical endocytic compartment; and (v) those non-opsonized *A. felis* that were taken up despite drug treatment were predominately delivered to a lysosomal compartment. In contrast, uptake of opsonized *A. felis* was not significantly affected by cholesterol depletion, cholesterol oxidase treatment or CTB addition, and phagosomes containing opsonized *A. felis* became LAMP1 positive (Table 1).

Lipid microdomains (lipid rafts) have been implicated in the uptake of a number of pathogenic bacteria such as *E. coli* (7), *Shigella flexneri* (13), *Listeria monocytogenes* (53), *Brucella suis* (14) or *Pseudomonas aeruginosa* (54). In most of these studies, entry of bacteria into non-professional phagocytic epithelial cells has been investigated while our study focuses on professional phagocytic macrophages which are endowed with a variety of receptors dedicated to recognize and bind foreign particles and to induce their ingestion: prime examples are receptors for mannose, immunoglobulin, complement factors, or lipopolysaccharide from Gram-negative or lipoteichoic acid from Gram-positive bacteria (55). Different receptors are likely to co-operate in binding and inducing uptake of bacteria that express on their surface a multitude of potential ligands. Lipid microdomains, though also present on some intracellular membranes, are mostly platforms

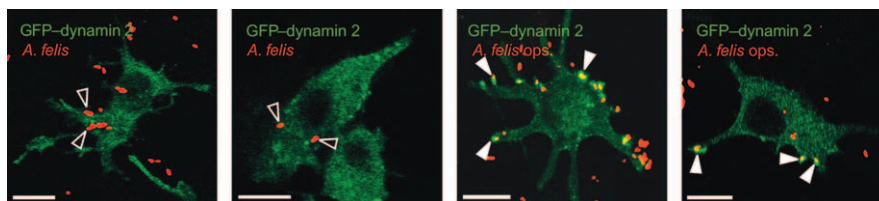


Figure 8: *A. felis* enters J774E macrophages into a compartment negative for dynamin-2. RAW 264.7 macrophages transiently expressing GFP-labeled dynamin-2 were infected with *A. felis* or with *A. felis* preincubated with monoclonal antibody ('ops.'). Optical overlays are shown. GFPs appear in green, bacteria in red and overlaps in yellow. Open arrows point to phagosomes containing non-opsonized *A. felis*, closed arrows to opsonized *A. felis*. Bars, 10 μ m.

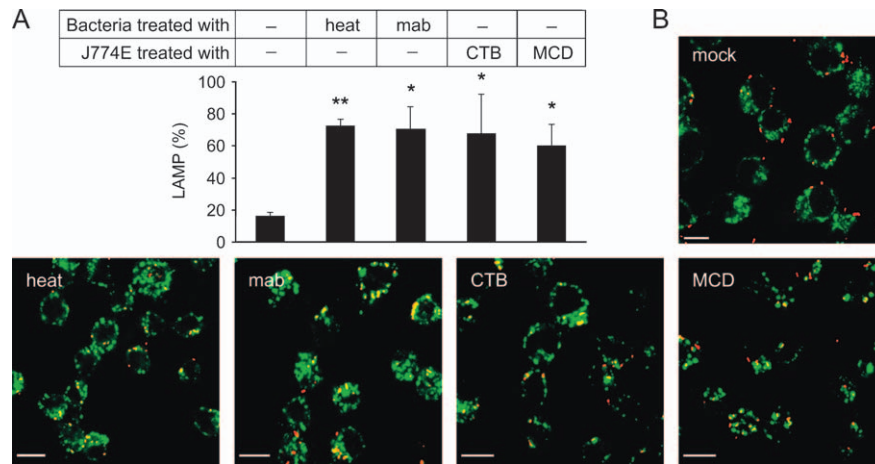


Figure 9: Final compartmentation of *A. felis*-containing phagosomes depends on port of entry. A) J774E macrophages were left untreated or treated with 10 μ g/mL CTB or 20 mM MCD as in Figure 3. Macrophages were infected with untreated, live *A. felis* ('untreated', 'CTB', 'MCD') or antibody-opsonized *A. felis* ('mab') or heat-killed *A. felis* ('heat'). Colocalization frequency of phagosomes with LAMP1 after a 3-h chase was determined by confocal microscopy and quantified (shown are means \pm SD from three independent experiments, 200 macrophages were counted per sample and experiment). Significances were * $p < 0.05$; ** $p < 0.01$. B) Fluorescence micrographs of samples as in A. Bars, 10 μ m.

that transduce signals from raft-embedded receptors into the cell. Clustering of several of the very small lipid microdomains is a prerequisite for signaling (8,9). Clustering

Table 1: Summary of experimental data^a

	Opsonized <i>A. felis</i>	Non-opsonized <i>A. felis</i>
Binding to macrophages	+++	++
Uptake by macrophages	+++	+
Induction of actin polymerization	++	+
Colocalization with TfR	+	+/-
ACV colocalization with LAMP1/ lysosomes at 2 h of infection	+++	+
Inhibition of uptake by CTB treatment	–	++
Inhibition of uptake by cholesterol oxidase treatment	–	++
Inhibition of uptake by cholesterol extraction	–	++
ACV colocalization with YFP- MyrPalm	+++	+++
Colocalization of ACV with DTxR (70 000 MW) added during infection	–	++
Bacteria in macropinocytic structures by transmission electron microscopy	–	+++
Inhibition of uptake in presence of amiloride	+/-	+++
Does macrophage treatment with amiloride reduce bacterial survival?	ND	++

^a+++ , excellent/very strong or more than 70%; ++, very good/strong or more than 30% and less than 70%; +, good/fair or more than 10% and less than 30%; –, poor or not detectable or between 0 and 10%; ND, not done.

of lipid microdomains has been shown for pathogenic *L. monocytogenes* on Vero epithelial cells (53) and we have extended this analysis by describing the presence of YFP-MyrPalm on phagosomes in macrophages containing harmless particles, i.e. a cloning laboratory strain of *E. coli* (Figure 4 and data not shown). These data suggest that lipid rafts may be incorporated into most, if not all, kinds of phagosomes. While this is very suggestive with respect to a general pathway of uptake via lipid microdomains, the mere presence of lipid microdomains in phagosomes does not in itself constitute evidence for their role in the uptake process. Phagosomes containing IgG-coated *A. felis* clearly contained lipid microdomains while cholesterol extraction and related treatments had very little effect on the ingestion of these bacteria by macrophages. Obviously, the presence of lipid rafts in phagosomes is not sufficient for assigning them a crucial role in the uptake machinery, but microdomains may also be fortuitously included when very large plasma membrane areas are invaginated and ingested. Alternatively, different lipid microdomain proteins may be differently susceptible to cholesterol extraction and modification. Such differential sensitivity has already been demonstrated in neutrophils: while the translocation of Fc γ RIIA receptor into detergent-resistant microdomains was not sensitive to MCD treatment, the constitutively microdomain-localized Src kinase Lyn was physically removed from this membrane fraction (56). This report is in good agreement with our findings and those of others (7,14) that the IgG-triggered pathway is rather insensitive to agents that disrupt lipid microdomain integrity, and that it can funnel the bacteria into the digestive lysosomal system, leading to a completely different phagosome compartmentation. This was elegantly demonstrated by Joiner et al. (57) using *Toxoplasma gondii* as a particle.

Ganglioside GM1 is the plasma membrane receptor for cholera toxin. The pentameric CTB mediates receptor binding and each of the five subunits engages one GM1 molecule. Availability of high concentrations of GM1 in lipid microdomains may be the reason for the preferred binding of cholera toxin to GM1 in these domains (28), which then leads to the internalization of the CTB–GM1 complex (58). Internalization may deplete the plasma membrane of domains required for *Afipia* uptake. GM1 was accumulated in phagosomes containing neither opsonized *A. felis* nor *E. coli*, and uptake of these bacteria by macrophages was independent of GM1 ligation. It is unlikely that *A. felis* uses GM1 itself as a receptor, as neither pretreatment of *A. felis* with pure GM1 before addition to macrophages nor increasing the plasma membrane GM1 content of GM1-deprived cells influenced binding or uptake of *Afipia* (data not shown).

Our study shows that both the kinetics of particle uptake and its fate can be influenced by opsonization: while non-opsonized *A. felis* entered macrophages very slowly and with weak and delayed actin polymerization, opsonized bacteria entered quickly and with robust local induction of actin polymerization. Similar to *A. felis*, *B. suis*, another intracellular pathogen, was taken up by macrophages very slowly, likely through macropinocytosis (see subsequently) and with disturbed actin polymerization (59). Notably, the resulting *Brucella*-containing vacuole is also an unusual, non-endocytic compartment. Similarly, uptake of *Legionella pneumophila* into bone-marrow-derived murine macrophages can occur by macropinocytosis. While wild-type *Legionella* was taken up slowly, a mutant in the virulence-mediating type IV secretion system was much faster ingested, and macropinocytosis was dependent on the secretion system (60).

Our further analysis showed that *A. felis* is taken up by macropinocytosis. The evidences for a crucial role of macropinocytosis in ACV development after uptake of non-opsonized *A. felis* were (i) electron microscopy showing *A. felis* entangled by numerous filopodia- and ruffle-like macrophage extensions while opsonized bacteria were taken up by a zipper-like mode; (ii) FM4-64 as a ubiquitous plasma membrane label or 70 000 MW DTxR as a fluid-phase label with preference for uptake via macropinosomes both labeled large subcellular bacteria-containing structures in the first minutes of infection while phagosomes containing opsonized bacteria were small when visualized with FM4-64 and they did not label at all with DTxR; (iii) the macropinocytosis inhibitor amiloride specifically inhibited uptake of non-opsonized bacteria; and (iv) wortmannin, an inhibitor of different types of endocytosis, including macropinocytosis, and cytochalasin (also inhibiting classical endocytosis, phagocytosis and macropinocytosis) inhibited uptake of either opsonized or non-opsonized *A. felis* (v) while only the non-opsonized *Afipia* were negative for TfR (Figure 2) or EEA1 (6) and their phagosomes did not mature into phagolysosomes (Table 1).

Macropinocytosis has, at least in some host cell types, been found to be the uptake mechanism for other pathogens, in particular of *Salmonella*, *Shigella*, *Brucella* and *Francisella* (15,44,48,61). Still, the molecular and functional characteristics of their vacuoles vary dramatically: while *Salmonella* localizes to a spacious late endocytic compartment which does not fuse with lysosomes and while *Brucella*-containing phagosomes are first part of the endocytic continuum but then branch off to become an endoplasmic-reticulum-like compartment, *Shigella* ruptures its vacuole to multiply in the host cell cytoplasm and *Legionella* inhabits an endoplasmic-reticulum-like compartment [all reviewed by Alonso and Garcia-del Portillo (24)]. Also, HIV-1 (41) is taken up into macrophages by macropinocytosis, a process which also requires plasma membrane microdomains (62).

Although amiloride has been frequently used as a powerful and specific inhibitor of macropinocytosis, very few studies have analyzed the step at which it inhibits the process. Dowrick et al. (18) noted, that amiloride inhibited ruffle formation in growth-hormone-treated epithelial MDCK cells. In our experiments with J774E cells, amiloride did not have a detectable inhibitory effect on ruffle formation, but rather seemed to arrest macropinosome production at a late stage, e.g. by inhibiting closure of the macropinocytic cups. This may be due to the fact that NHE-1, the target of amiloride, interacts with ezrin, an actin-binding protein that also binds to and activates type I PI(3) kinases (63). PI(3) kinase activity is required for the closure of nascent macropinosomes and phagosomes (45). Therefore, inhibition of NHE-1 by amiloride may indirectly affect PI(3) kinase function and membrane closure function. In the presence of amiloride, unconsumed pseudopodia would accumulate, thus leading to a quantitative difference in ruffle formation.

Macropinosomes are formed from fusing membrane ruffles. Areas of membrane ruffling seem to be enriched in lipid microdomains (64) and depletion of cholesterol from the plasma membrane inhibits membrane ruffling and macropinocytosis of ricin in A431 cells (38). We propose that non-opsonized *A. felis* facilitates its uptake via macropinocytosis by attaching to defined lipid microdomains that are predominately incorporated into macropinocytic vesicles. *Afipia felis* likely does not trigger macropinocytosis, but is rather a passive hitchhiker, as *Afipia*-infected macrophages did not seem to have more ruffle-like attachments than uninfected macrophages. The hypothesis that lipid microdomain engagement by *A. felis* and subsequent macropinocytic uptake are linked is supported by the facts that (i) the reduction in *A. felis* uptake by amiloride was approximately the same as the inhibition through cholesterol extraction and (ii) uptake of 70 000 MW DTxR was inhibited by cholesterol extraction just as uptake of *A. felis* was. Furthermore, the ultrastructural evidence clearly indicated that *A. felis* was enclosed in macropinocytic structures.

Engagement of the macropinosome-forming plasma membrane domains by *A. felis* might explain the unusual compartmentation of ACVs. There are at least two different modes of macropinocytosis: the processive mode which forwards the ingested substances into the endolysosomal system and the recycling mode which leads to the formation of macropinosomes that do not fuse with lysosomes (16,65,66). Notably, the processive mode has been reported to be predominant in macrophages, and should feed into the lysosomes (67). But J774E cells are also able to form macropinosomes that do not seem to mature into late endocytic organelles (17) and these may be identical to the *A. felis*-ingesting ones. On the other hand, *A. felis*-containing macropinosomes shrink within minutes after formation and the bacteria become separated from the bulk macropinosomal content. This was visualized using 70 000 MW DTxR, which is delivered to a LAMP1-positive compartment (data not shown), regardless of whether *A. felis* was part of it or not. It might be possible that *A. felis* actively influences its fate after the uptake process, e.g. by secretion of effector proteins. In line with such a hypothesis, the uptake of heat-killed *Afipia* by macrophages was also inhibited by amiloride and the early phagosomes containing heat-killed *Afipia* were negative for TfR as well (data not shown), suggesting the usage of an identical port of entry by *A. felis* and an active role of live *A. felis* in subsequent trafficking decisions. Macropinocytic uptake of *Afipia* seemed to be required for subverting lysosomal trafficking as IgG opsonization or blocking the macropinocytic entry pathway lead to normalized phagosome maturation.

In agreement with macropinocytosis as the major uptake mode for *A. felis*, the ACV is likely not a product of caveolae-mediated uptake, as we could not detect any GFP-caveolin-1 on ACVs at any time tested (data not shown) and as dynamin-2 did not colocalize with non-opsonized *A. felis*. Furthermore, we did not find a significantly enhanced colocalization rate of non-opsonized versus opsonized *A. felis* with simian virus 40 virions that are marker particles for caveosomes [(68); data not shown]. The ACV is also not likely the result of uptake via an alternative flotillin1-dependent pathway or a non-clathrin route of entry for GPI-anchored proteins (69), as flotillin1 clearly did not colocalize to ACVs during the first hour of infection, and neither did CD14, a paradigm macrophage GPI-anchored protein (70) (data not shown). Finally, the fully developed ACV was not accessible for fluid-phase markers such as 10 000 MW dextran (Figure 2A) or ovalbumin (6) fed into the endocytic system and does not contain any of the canonical endocytic marker molecules tested, such as Rab5 or Rab7, EEA1, TfR, VAMP8, mannose 6-phosphate receptor, LAMP1 and LAMP2, vacuolar ATPase complex, β -glucuronidase, cathepsin D and others (6). Our data show that *A. felis* localized to this unusual compartment only if not opsonized and that it was delivered to late endocytic compartments if it was opsonized before infection or if entry via lipid-raft-mediated

macropinocytosis was blocked by drug treatment. Together with the previous findings in other infection systems (*Brucella*, *Legionella*, *Francisella*, *Salmonella*), our data suggest the existence of several different macropinocytic entry ways, at least some of which are slow, require lipid microdomain integrity and function, and whose macropinosomes shrink within a matter of minutes (17,60). Such macropinosomes are hitchhiked by *A. felis*. Therefore, *A. felis* can be used as a novel tool to study a particular macropinocytic uptake pathway and its role in bacteria infection.

Materials and Methods

Cell culture and bacteria

Murine macrophage-like cell lines J774E (from P.D. Stahl, Washington University, St Louis, MO, USA) and RAW 264.7 (from H. Hilbi, ETH Zürich, Zurich, Switzerland) were grown in DMEM (Sigma, Taufkirchen, Germany)/10% fetal calf serum (FCS) (Gibco, Karlsruhe, Germany)/Glutamax (Gibco) media (37°C/7% CO₂). Type strain of *A. felis* (ATCC 53690) was from the Deutsche Sammlung von Mikroorganismen und Zellkulturen (Braunschweig, Germany; DSM 7326) and grown as described by Lührmann et al. (6), and *E. coli* DH5 α from Promega (Mannheim, Germany) were grown in Luria Broth at 37°C.

Antibodies

Monoclonal rat antibodies to TfR (clone TIB 219) and monoclonal rat anti-LAMP1 (clone D4B) antibodies were gifts from U.E. Schaible (Berlin, Germany). Rabbit anti-*Afipia* spp. or anti-*E. coli* DH5 α were from our laboratory. Monoclonal mouse anti-*A. felis* (clone 1A5-5, subtype IgG3a, titer 1:16 000) was a kind gift from D. Raoult (Faculté de Médecine, Marseille, France (71)). Secondary antibodies were goat anti-rabbit IgG Alexa Fluor 488 (A-11008, Molecular Probes, Eugene, OR, USA), donkey anti-rabbit IgG Cy3 (711-165-152, Jackson via Dianova, Hamburg, Germany), goat anti-mouse IgG Alexa Fluor 488 (A-11001, Molecular Probes), donkey anti-mouse IgG Cy3 (715-165-152, Jackson via Dianova), and goat anti-rat IgG Alexa Fluor 488 (A-11006, Molecular Probes).

Infection and immunofluorescence analysis

The day before infection, 3×10^5 macrophages per well were seeded onto coverslips in a 24-well plate (all cell culture plasticware was from TPP, Trasadingen, Switzerland). J774E were infected with *A. felis* [multiplicity of infection (MOI) 100], opsonized *A. felis* (MOI 10) or *E. coli* (MOI 50) in serum-free medium by centrifugation for 5 min at $500 \times g$ at 15°C to synchronize uptake. *Afipia felis* was opsonized in 1% 1A5-5 for 30 min at room temperature. Cells were extensively rinsed with phosphate-buffered saline (PBS), and incubated in fresh medium at 37°C for the indicated times. To account for kinetic differences in uptake of opsonized versus non-opsonized *A. felis*, we followed colocalization of *A. felis* and the early markers, TfR, actin and dynamin-2 for at least 1 h to ensure that differences in colocalization were not due to a delayed uptake.

For microscopic analysis, coverslips were rinsed with PBS and fixed in 3% formaldehyde in PBS for 25 min at room temperature, followed by a 20-min incubation with 50 mM NH₄Cl in PBS. Permeabilization was for 10 min in permeabilization buffer (PB, 0.1% TX-100 in PBS containing 5% goat or donkey serum). Specific primary and fluorophore-conjugated secondary antibodies were diluted in TX-100-free PB, added to coverslips in a humidified chamber and incubated for 45 min at room temperature. Following two final washes, coverslips were rinsed in bidistilled water and mounted in Mowiol. Filamentous actin was visualized using phalloidin conjugated to Alexa Fluor 488 (A-12379, Molecular Probes) at a concentration of 0.25 U per sample. GM1 was detected using biotinylated CTB (5 μ g/mL), followed

by incubation with avidin–fluorescein isothiocyanate (0.1 mg/mL, 50 μ L per sample). Plasma membrane staining was performed using the lipophilic styryl dye FM4-64 (T-13320, Molecular Probes) which was present during infections in a concentration of 5 μ g/mL. Samples were analyzed using a confocal laser scanning microscope (LSM 510, Zeiss, Oberkochen, Germany). To distinguish intracellular from extracellular bacteria, differential antibody staining was performed: extracellular bacteria were labeled without permeabilization using specific primary antibody and Cy3-conjugated goat anti-rabbit in experiments with *A. felis* or *E. coli* or using goat anti-mouse in experiments with opsonized *A. felis*. Intracellular bacteria were then stained using the same primary antibodies but in the presence of 0.1% TX-100/PBS for 10 min, followed by Alexa Fluor 488-conjugated goat anti-rabbit in *A. felis* or *E. coli* experiments, or goat anti-mouse for opsonized *A. felis*.

Accessibility of phagosomes to DTxR

Infection was performed as described for *A. felis* or opsonized *A. felis*. Cells were chased for 30, 60 or 120 min, followed by a 2-h chase with fresh medium containing 0.15 mg/mL DTxR 10 000 MW (Molecular Probes). After fixing the samples as described, bacteria were labeled with specific antibodies and colocalization with DTxR was quantified by laser scanning microscopy. DTxR 70 000 MW was used to study the process of macropinocytosis and to track macropinocytotic vesicles inside the cells. J774E were infected with opsonized (MOI 5) or non-opsonized (MOI 50) *A. felis* in the presence of 0.4 mg/mL DTxR (70 000 MW) in serum-free media for 30 min, rinsed three times with PBS and either fixed immediately or chased for another 30 min in fresh medium without tracer. Bacteria were labeled using specific antibodies and analyzed for colocalization with DTxR by laser scanning microscopy.

Drug treatment and infection experiments

The day before infection, J774E were seeded either onto plastic or onto coverslips in a 24-well plate (3×10^5 cells/well). Cells were treated in a 300- μ L volume with the indicated quantities of CTB (C9972, Sigma) or MCD (C4555, Sigma) for 30 min, or cholesterol oxidase (228230, Calbiochem, Darmstadt, Germany) for 60 min in DMEM lacking FCS. Samples were rinsed once with PBS and fresh medium was added. *A. felis* (MOI 200), opsonized *A. felis* (MOI 50) or *E. coli* (MOI 100) were added for 90 min at 37°C/7% CO₂. To quantify the number of intracellular bacteria, a gentamicin protection assay was performed: cells were rinsed three times with warm PBS after infection and incubated for 1 h at 37°C/5% CO₂ in medium containing 300 μ g/mL gentamicin to kill extracellular bacteria. Macrophages were rinsed once with warm PBS and then lysed in ice-cold bidistilled water. Samples were diluted and plated on buffered charcoal yeast extract (*A. felis*) or Luria Broth (*E. coli*) nutrient agar plates to quantify colony-forming units. To quantify the colocalization of *A. felis* with LAMP1 after drug treatment, cells were infected with *A. felis* (MOI 200) for 30 min. Where indicated, *A. felis* were first killed by heating for 15 min at 80°C. After rinsing cells extensively with PBS, fresh medium was added and cells were incubated for 3 h at 37°C/7% CO₂ and processed for fluorescence microscopy as described above.

To analyze the role of macropinocytosis, cells were preincubated with the indicated concentrations of amiloride (A7419, Sigma), 100 nm wortmannin (W1628, Sigma) or 1 μ M cytochalasin D (C8273, Sigma) for 10 min and subsequently infected with *A. felis* (MOI 50) or opsonized *A. felis* (MOI 5) in the presence of the respective drug for 30 min at 37°C/7% CO₂. Cells were rinsed three times with warm PBS and prepared for differential antibody staining as described.

Preparation of MCD–cholesterol complexes and cholesterol repletion

According to Klein et al. (72), 6 mg cholesterol (C8667, Sigma) was dissolved in 80 μ L of isopropanol:chloroform (2:1), added dropwise to a solution of 200 mg MCD in 2.2 mL bidest at 80°C with stirring, yielding a solution of 6.8 mM cholesterol. MCD–cholesterol complexes were diluted to a final concentration of 0.2 mM into serum-free DMEM medium

containing 1 mg/mL bovine BSA and added to MCD-treated cells for 30 min at 37°C. Samples were rinsed once with PBS, medium was added and infection with *A. felis* (MOI 200) was performed as described above, followed by a gentamicin protection assay.

Transfection of RAW 264.7 cells and cold TX-100 extraction

RAW 264.7 cells (easier to transfect than J774E cells) were transfected by electroporation (Multiporator, Eppendorf, Hamburg, Germany) according to the manufacturer's protocol. Briefly, cells from exponential growth phase were rinsed with DMEM/0.5% FCS and resuspended in Eppendorf Hypoosmolar Electroporation Buffer (no. 4308070.501, Eppendorf) at 5×10^6 cells/mL. Plasmid DNA (30 μ g/mL; GenElute endotoxin-free plasmid midiprep kit, PLED-35, Sigma) was added; 800 μ L of the suspension was transferred into an electroporation cuvette (4 mm gap width, Eppendorf) and treated with 570 V for 50 μ seconds. Cells were allowed to sit for 5–10 min at room temperature, transferred to DMEM/10% FCS and seeded onto coverslips in a 24-well plate at a concentration of 3×10^5 cells/well. Experiments were done the day after transfection. The plasmids encoding 'YFP-MyrPalm' and 'YFP-GerGer' (35) were kind gifts from R. Tsien (UCSD, San Diego, CA, USA), GFP-dynamin-2 (73) was generously provided by M. McNiven (Mayo Clinic, Rochester, MN, USA) and the GFP–caveolin-1 construct was from R. Parton (University of Queensland, Australia). In TX-100 extraction experiments, coverslips were rinsed with PBS and incubated for 30 min at 4°C with PBS only or with PBS containing 1% TX-100 (as indicated), followed by sample preparation for fluorescence microscopy.

Electron microscopy

To examine the ultrastructure of uptake of *A. felis* or opsonized *A. felis* by J774E, cells were seeded in six-well plates the day before infection (1×10^6 per well). After infection with non-opsonized (MOI 1000) or opsonized (MOI 100) *A. felis* after centrifugation as above, medium was replaced by 37°C fresh medium and plates were further incubated at 37°C for 1, 10 or 30 min, as indicated. At the indicated times, cells were rinsed three times with PBS and fixed in 0.25% glutaraldehyde/2% formaldehyde in PBS for 2 h at room temperature. Samples were rinsed with distilled water and stained in 1.5% potassium ferricyanide/1% osmium tetroxide in distilled water at 4°C for 60 min, followed by extensive rinsing with distilled water. Samples were incubated in 4% uranyl acetate in aqua dest. for 60 min at 4°C, followed by 3 min in aqua dest. After incubation in 0.1% tannic acid in aqua dest. for 30 min at room temperature, cells were rinsed with distilled water, dehydrated using standard ethanol dilution series, scraped off the culture dishes and placed into microfuge tubes. The samples were embedded in Epon; thin sections were collected on nickel grids and examined using a Philips CM 120 transmission electron microscope.

Acknowledgments

The authors thank Drs Kristin Birkness, Hubert Hilbi, Mark Marsh, Mark McNiven, Robert Parton, Fred Quinn, Didier Raoult, Ulrich Schaible, Philip Stahl and Roger Tsien for generous gifts of reagents, strains and advice. Expert technical assistance by Stephanie Schielke and Sabine Spürck was highly appreciated. Financial support through the Deutsche Forschungsgemeinschaft (HA1929/6-2) and initial support through a research award from American Gene Therapy Inc. (special thanks to Prof. Aladar Szalay) are gratefully acknowledged.

References

1. Haas A. The phagosome: compartment with a license to kill. *Traffic*, in press.
2. Scott CC, Botelho RJ, Grinstein S. Phagosome maturation: a few bugs in the system. *J Membr Biol* 2003;193:137–152.

3. Brenner DJ, Hollis DG, Moss CW, English CK, Hall GS, Vincent J, Radosevic J, Birkness KA, Bibb WF, Quinn FD, Swaminathan B, Weaver RE, Reeves MW, O'Connor SP, Hayes PS et al. Proposal of *Afipia* gen. nov., with *Afipia felis* sp. nov. (formerly the cat scratch disease bacillus), *Afipia clevelandensis* sp. nov. (formerly the Cleveland Clinic Foundation strain), *Afipia broomeae* sp. nov., and three unnamed genospecies. *J Clin Microbiol* 1991;29:2450–2460.
4. Giladi M, Avidor B, Kletter Y, Abulafia S, Slater LN, Welch DF, Brenner DJ, Steigerwalt AG, Whitney AM, Ephros M. Cat scratch disease: the rare role of *Afipia felis*. *J Clin Microbiol* 1998;36:2499–2502.
5. Lührmann A, Haas A. A method to purify bacteria-containing phagosomes from infected macrophages. *Methods Cell Sci* 2000;22:329–341.
6. Lührmann A, Streker K, Schüttfort A, Daniels JJ, Haas A. *Afipia felis* induces uptake by macrophages directly into a nonendocytic compartment. *Proc Natl Acad Sci U S A* 2001;98:7271–7276.
7. Baorto DM, Gao Z, Malaviya R, Dustin ML, van der Merwe A, Lublin DM, Abraham SN. Survival of FimH-expressing enterobacteria in macrophages relies on glycolipid traffic. *Nature* 1997;389:636–639.
8. Nichols BJ. GM1-containing lipid rafts are depleted within clathrin-coated pits. *Curr Biol* 2003;13:686–690.
9. Rajendran L, Simons K. Lipid rafts and membrane dynamics. *J Cell Sci* 2005;118:1099–1102.
10. Guan JL. Cell biology. Integrins, rafts, Rac, and Rho. *Science* 2004;303:773–774.
11. Peyron P, Bordier C, N'Diaye EN, Maridonneau-Parini I. Nonopsonic phagocytosis of *Mycobacterium kansasii* by human neutrophils depends on cholesterol and is mediated by CR3 associated with glycosylphosphatidylinositol-anchored proteins. *J Immunol* 2000;165:5186–5191.
12. Watarai M, Makino S, Michikawa M, Yanagisawa K, Murakami S, Shirahata T. Macrophage plasma membrane cholesterol contributes to *Brucella abortus* infection of mice. *Infect Immun* 2002;70:4818–4825.
13. Lafont F, Tran Van Nhieu G, Hanada K, Sansonetti P, van der Goot FG. Initial steps of *Shigella* infection depend on the cholesterol/sphingolipid raft-mediated CD44-IpaB interaction. *EMBO J* 2002;21:4449–4457.
14. Naroeni A, Porte F. Role of cholesterol and the ganglioside GM(1) in entry and short-term survival of *Brucella suis* in murine macrophages. *Infect Immun* 2002;70:1640–1644.
15. Watarai M, Makino S, Fujii Y, Okamoto K, Shirahata T. Modulation of *Brucella*-induced macropinocytosis by lipid rafts mediates intracellular replication. *Cell Microbiol* 2002;4:341–355.
16. Swanson JA, Watts C. Macropinocytosis. *Trends Cell Biol* 1995;5:424–428.
17. Albrecht I, Gatfield J, Mini T, Jenö P, Pieters J. Essential role for cholesterol in the delivery of exogenous antigens to the MHC class I-presentation pathway. *Int Immunol* 2006;18:755–765.
18. Dowrick P, Kenworthy P, McCann B, Warn R. Circular ruffle formation and closure lead to macropinocytosis in hepatocyte growth factor/scatter factor-treated cells. *Eur J Cell Biol* 1993;61:44–53.
19. West MA, Antoniou AN, Prescott AR, Azuma T, Kwiatkowski DJ, Watts C. Membrane ruffling, macropinocytosis and antigen presentation in the absence of gelsolin in murine dendritic cells. *Eur J Immunol* 1999;29:3450–3455.
20. Leitinger B, Hogg N. The involvement of lipid rafts in the regulation of integrin function. *J Cell Sci* 2002;115:963–972.
21. Damm EM, Pelkmans L, Kartenbeck J, Mezzacasa A, Kurzchalia T, Helenius A. Clathrin- and caveolin-1-independent endocytosis: entry of simian virus 40 into cells devoid of caveolae. *J Cell Biol* 2005;168:477–488.
22. Fernandez-Mora E, Polidori M, Lührmann A, Schaible UE, Haas A. Maturation of *Rhodococcus equi*-containing vacuoles is arrested after completion of the early endosome stage. *Traffic* 2005;6:635–653.
23. Vieira OV, Botelho RJ, Grinstein S. Phagosome maturation: aging gracefully. *Biochem J* 2002;366:689–704.
24. Alonso A, Garcia-del Portillo F. Hijacking of eukaryotic functions by intracellular bacterial pathogens. *Int Microbiol* 2004;7:181–191.
25. Duncan MJ, Li G, Shin JS, Carson JL, Abraham SN. Bacterial penetration of bladder epithelium through lipid rafts. *J Biol Chem* 2004;279:18944–18951.
26. Manes S, del Real G, Martinez AC. Pathogens: raft hijackers. *Nat Rev Immunol* 2003;3:557–568.
27. Badizadegan K, Wolf AA, Rodighiero C, Jobling M, Hirst TR, Holmes RK, Lencer WI. Floating cholera toxin into epithelial cells: functional association with caveolae-like detergent-insoluble membrane microdomains. *Int J Med Microbiol* 2000;290:403–408.
28. Schiavo G, van der Goot FG. The bacterial toxin toolkit. *Nat Rev Mol Cell Biol* 2001;2:530–537.
29. Kilsdonk EP, Yancey PG, Stoudt GW, Bangerter FW, Johnson WJ, Phillips MC, Rothblat GH. Cellular cholesterol efflux mediated by cyclodextrins. *J Biol Chem* 1995;270:17250–17256.
30. Masserini M, Ravasi D. Role of sphingolipids in the biogenesis of membrane domains. *Biochim Biophys Acta* 2001;1532:149–161.
31. Rouquette-Jazdarian AK, Pelassy C, Breittmayer JP, Aussel C. Reevaluation of the role of cholesterol in stabilizing rafts implicated in T cell receptor signaling. *Cell Signal* 2006;18:105–122.
32. Wood WG, Igbavboa U, Rao AM, Schroeder F, Avdulov NA. Cholesterol oxidation reduces Ca^{2+} + Mg^{2+} -ATPase activity, interdigitation, and increases fluidity of brain synaptic plasma membranes. *Brain Res* 1995;683:36–42.
33. Ulloa JE, Casiano CA, De Leon M. Palmitic and stearic fatty acids induce caspase-dependent and -independent cell death in nerve growth factor differentiated PC12 cells. *J Neurochem* 2003;84:655–668.
34. Lafont F, Abrami L, van der Goot FG. Bacterial subversion of lipid rafts. *Curr Opin Microbiol* 2004;7:4–10.
35. Zacharias DA, Violin JD, Newton AC, Tsien RY. Partitioning of lipid-modified monomeric GFPs into membrane microdomains of live cells. *Science* 2002;296:913–916.
36. Simons K, Toomre D. Lipid rafts and signal transduction. *Nat Rev Mol Cell Biol* 2000;1:31–39.
37. Munro S. Lipid rafts: elusive or illusive? *Cell* 2003;115:377–388.
38. Grimmer S, van Deurs B, Sandvig K. Membrane ruffling and macropinocytosis in A431 cells require cholesterol. *J Cell Sci* 2002;115:2953–2962.
39. Alpuche-Aranda CM, Racoosin EL, Swanson JA, Miller SI. *Salmonella* stimulate macrophage macropinocytosis and persist within spacious phagosomes. *J Exp Med* 1994;179:601–608.
40. West MA, Bretscher MS, Watts C. Distinct endocytotic pathways in epidermal growth factor-stimulated human carcinoma A431 cells. *J Cell Biol* 1989;109:2731–2739.
41. Marechal V, Prevost MC, Petit C, Perret E, Heard JM, Schwartz O. Human immunodeficiency virus type 1 entry into macrophages mediated by macropinocytosis. *J Virol* 2001;75:11166–11177.
42. Harris C, Fliegel L. Amiloride and the Na(+)/H(+) exchanger protein: mechanism and significance of inhibition of the Na(+)/H(+) exchanger (review). *Int J Mol Med* 1999;3:315–321.
43. Noguchi H, Matsumoto S, Okitsu T, Iwanaga Y, Yonekawa Y, Nagata H, Matsushita M, Wei FY, Matsui H, Minami K, Seino S, Masui Y, Futaki S, Tanaka K. PDX-1 protein is internalized by lipid raft-dependent macropinocytosis. *Cell Transplant* 2005;14:637–645.
44. Clemens DL, Lee BY, Horwitz MA. *Francisella tularensis* enters macrophages via a novel process involving pseudopod loops. *Infect Immun* 2005;73:5892–5902.
45. Araki N, Johnson MT, Swanson JA. A role for phosphoinositide 3-kinase in the completion of macropinocytosis and phagocytosis by macrophages. *J Cell Biol* 1996;135:1249–1260.

46. Simonsen A, Wurmser AE, Emr SD, Stenmark H. The role of phosphoinositides in membrane transport. *Curr Opin Cell Biol* 2001;13:485–492.
47. Sieczkarski SB, Whittaker GR. Dissecting virus entry via endocytosis. *J Gen Virol* 2002;83:1535–1545.
48. Gold ES, Underhill DM, Morrissette NS, Guo J, McNiven MA, Aderem A. Dynamin 2 is required for phagocytosis in macrophages. *J Exp Med* 1999;190:1849–1856.
49. Orth JD, Krueger EV, Cao H, McNiven MA. The large GTPase dynamin regulates actin comet formation and movement in living cells. *Proc Natl Acad Sci U S A* 2002;99:167–172.
50. Di A, Nelson DJ, Bindokas V, Brown ME, Libunao F, Palfrey HC. Dynamin regulates focal exocytosis in phagocytosing macrophages. *Mol Biol Cell* 2003;14:2016–2028.
51. Smith AE, Helenius A. How viruses enter animal cells. *Science* 2004;304:237–242.
52. Pelkmans L, Helenius A. Insider information: what viruses tell us about endocytosis. *Curr Opin Cell Biol* 2003;15:414–422.
53. Seveau S, Bierne H, Giroux S, Prevost MC, Cossart P. Role of lipid rafts in E-cadherin- and HGF-R/Met-mediated entry of *Listeria monocytogenes* into host cells. *J Cell Biol* 2004;166:743–753.
54. Grassme H, Jendrossek V, Riehle A, von Kurthy G, Berger J, Schwarz H, Weller M, Kolesnick R, Gulbins E. Host defense against *Pseudomonas aeruginosa* requires ceramide-rich membrane rafts. *Nat Med* 2003;9:322–330.
55. Stuart LM, Ezekowitz RA. Phagocytosis: elegant complexity. *Immunity* 2005;22:539–550.
56. Rollet-Labelle E, Marois S, Barbeau K, Malawista SE, Naccache PH. Recruitment of the cross-linked opsonic receptor CD32A (FcγRIIA) to high-density detergent-resistant membrane domains in human neutrophils. *Biochem J* 2004;381:919–928.
57. Joiner KA, Fuhrman SA, Miettinen HM, Kasper LH, Mellman I. *Toxoplasma gondii*: fusion competence of parasitophorous vacuoles in Fc receptor-transfected fibroblasts. *Science* 1990;249:641–646.
58. Montesano R, Roth J, Robert A, Orci L. Non-coated membrane invaginations are involved in binding and internalization of cholera and tetanus toxins. *Nature* 1982;296:651–653.
59. Arellano-Reynoso B, Lapaque N, Salcedo S, Briones G, Ciocchini AE, Ugalde R, Moreno E, Moriyon I, Gorvel JP. Cyclic beta-1,2-glucan is a *Brucella* virulence factor required for intracellular survival. *Nat Immunol* 2005;6:618–625.
60. Watarai M, Derre I, Kirby J, Growney JD, Dietrich WF, Isberg RR. *Legionella pneumophila* is internalized by a macropinocytotic uptake pathway controlled by the Dot/Icm system and the mouse Lgn1 locus. *J Exp Med* 2001;194:1081–1096.
61. Amyere M, Mettlen M, Van Der Smissen P, Platek A, Payrastra B, Veithen A, Courtoy PJ. Origin, originality, functions, subversions and molecular signalling of macropinocytosis. *Int J Med Microbiol* 2002;291:487–494.
62. Liu NQ, Lossinsky AS, Popik W, Li X, Gujuluva C, Kriederman B, Roberts J, Pushkarsky T, Bukrinsky M, Witte M, Weinand M, Fiala M. Human immunodeficiency virus type 1 enters brain microvascular endothelia by macropinocytosis dependent on lipid rafts and the mitogen-activated protein kinase signaling pathway. *J Virol* 2002;76:6689–6700.
63. Gautreau A, Pouillet P, Louvard D, Arpin M. Ezrin, a plasma membrane-microfilament linker, signals cell survival through the phosphatidylinositol 3-kinase/Akt pathway. *Proc Natl Acad Sci U S A* 1999;96:7300–7305.
64. Nichols BJ, Lippincott-Schwartz J. Endocytosis without clathrin coats. *Trends Cell Biol* 2001;11:406–412.
65. Hewlett LJ, Prescott AR, Watts C. The coated pit and macropinocytic pathways serve distinct endosome populations. *J Cell Biol* 1994;124:689–703.
66. Maniak M. Macropinocytosis. In: Marsh M., editor. *Frontiers in Molecular Biology: Endocytosis*. New York: Oxford University Press; 2001, pp. 78–93.
67. Racoosin EL, Swanson JA. Macropinosome maturation and fusion with tubular lysosomes in macrophages. *J Cell Biol* 1993;121:1011–1020.
68. Pelkmans L, Kartenbeck J, Helenius A. Caveolar endocytosis of simian virus 40 reveals a new two-step vesicular-transport pathway to the ER. *Nat Cell Biol* 2001;3:473–483.
69. Glebov OO, Bright NA, Nichols BJ. Flotillin-1 defines a clathrin-independent endocytic pathway in mammalian cells. *Nat Cell Biol* 2006;8:46–54.
70. Sabharanjak S, Sharma P, Parton RG, Mayor S. GPI-anchored proteins are delivered to recycling endosomes via a distinct cdc42-regulated, clathrin-independent pinocytic pathway. *Dev Cell* 2002;2:411–423.
71. Yu X, Raouf D. Monoclonal antibodies to *Afipia felis* – a putative agent of cat scratch disease. *Am J Clin Pathol* 1994;101:603–606.
72. Klein U, Gimpl G, Fahrenholz F. Alteration of the myometrial plasma membrane cholesterol content with beta-cyclodextrin modulates the binding affinity of the oxytocin receptor. *Biochemistry* 1995;34:13784–13793.
73. Thompson HM, Cao H, Chen J, Euteneuer U, McNiven MA. Dynamin 2 binds gamma-tubulin and participates in centrosome cohesion. *Nat Cell Biol* 2004;6:335–342.